(12) INTERNATIONAL APPLICATION PUBLISHED UNDER THE PATENT COOPERATION TREATY (PCT)

(19) World Intellectual Property Organization
International Bureau

(43) International Publication Date
3 March 2016 (03.03.2016)

WIPO | PCT

(10) International Publication Number
WO 2016/030749 A1

(51) International Patent Classification:
C25B 11/04 (2006.01) *C25B 3/04* (2006.01)

(21) International Application Number:
PCT/IB2015/001687

(22) International Filing Date:
28 August 2015 (28.08.2015)

(25) Filing Language: English

(26) Publication Language: English

(30) Priority Data:
62/043,444 29 August 2014 (29.08.2014) US

(71) Applicants: **KING ABDULLAH UNIVERSITY OF SCIENCE AND TECHNOLOGY** [SA/SA]; 4700 King Abdulaah University of Science And Technology, Thuwal, 23955-6900 (SA). **SAUDI ARAMCO** [SA/SA]; Dhahran 31311 (SA).

(72) Inventors: **TAKANABE, Kazuhiro**; 4700 King Abdullah University of Science and Technology, Thuwal, 23955-6900 (SA). **RASUL, Shahid**; 4700 King Abdullah University of Science and Technology, Thuwal, 23955-6900 (SA). **EPPINGER, Jorg**; 4700 King Abdullah University of Science and Technology, Thuwal, 23955-6900 (SA). **OCHSENKUHN, Michael**; 4700 King Abdullah University of Science and Technology, Thuwal, 23955-6900 (SA). **ALROWAIHI, Israa, Salem**; 4700 King Abdullah University of Science and Technology, Thuwal, 23955-6900 (SA).

(81) Designated States *(unless otherwise indicated, for every kind of national protection available)*: AE, AG, AL, AM, AO, AT, AU, AZ, BA, BB, BG, BH, BN, BR, BW, BY, BZ, CA, CH, CL, CN, CO, CR, CU, CZ, DE, DK, DM, DO, DZ, EC, EE, EG, ES, FI, GB, GD, GE, GH, GM, GT, HN, HR, HU, ID, IL, IN, IR, IS, JP, KE, KG, KN, KP, KR, KZ, LA, LC, LK, LR, LS, LU, LY, MA, MD, ME, MG, MK, MN, MW, MX, MY, MZ, NA, NG, NI, NO, NZ, OM, PA, PE, PG, PH, PL, PT, QA, RO, RS, RU, RW, SA, SC, SD, SE, SG, SK, SL, SM, ST, SV, SY, TH, TJ, TM, TN, TR, TT, TZ, UA, UG, US, UZ, VC, VN, ZA, ZM, ZW.

(84) Designated States *(unless otherwise indicated, for every kind of regional protection available)*: ARIPO (BW, GH, GM, KE, LR, LS, MW, MZ, NA, RW, SD, SL, ST, SZ, TZ, UG, ZM, ZW), Eurasian (AM, AZ, BY, KG, KZ, RU, TJ, TM), European (AL, AT, BE, BG, CH, CY, CZ, DE, DK, EE, ES, FI, FR, GB, GR, HR, HU, IE, IS, IT, LT, LU, LV, MC, MK, MT, NL, NO, PL, PT, RO, RS, SE, SI, SK, SM, TR), OAPI (BF, BJ, CF, CG, CI, CM, GA, GN, GQ, GW, KM, ML, MR, NE, SN, TD, TG).

Declarations under Rule 4.17:

— *as to applicant's entitlement to apply for and be granted a patent (Rule 4.17(ii))*

— *as to the applicant's entitlement to claim the priority of the earlier application (Rule 4.17(iii))*

Published:

— *with international search report (Art. 21(3))*

WO 2016/030749 A1

(54) **Title**: ELECTRODES, METHODS OF MAKING ELECTRODES, AND METHODS OF USING ELECTRODES

(57) **Abstract**: Embodiments of the present disclosure provide for converting CO_2 to CO and formic acid, electrodes, devices including electrodes, methods of making electrodes, and the like.

ELECTRODES, METHODS OF MAKING ELECTRODES, AND METHODS OF USING ELECTRODES

CLAIM OF PRIORITY TO RELATED APPLICATION

This application claims priority to co-pending U.S. provisional application entitled "ELECTRODES, METHODS OF MAKING ELECTRODES, AND METHODS OF USING ELECTRODES" having Serial No.: 62/043,444, filed on August 29, 2014, which is entirely incorporated herein by reference.

BACKGROUND

The electricity generated from renewable resources, such as wind, geothermal, and photovoltaic technologies can convert atmospheric/industrially sourced carbon dioxide generated in refineries and power plants, where there is a significant potential to not only ensure the protection of the environment but also safeguard global economic security. The direct formation of CO_2 reduction products in electrochemical cells can provide a continuous supply of high-energy carrier fuels at small/medium scales. The construction of the electrocatalysts that can efficiently activate stable CO_2 molecules to specific product with high selectivity has proven to be a significant challenge.

SUMMARY

Embodiments of the present disclosure provide for converting CO_2 to CO and formic acid, electrodes, devices including electrodes, methods of making electrodes, and the like.

An embodiment of the present disclosure provides a method of converting CO_2 to CO and formic acid, among others, that includes: exposing CO_2 and H_2O to a cathode to form formic acid and O_2 at an anode, wherein the cathode includes a substrate having a material thereon. The material thereon can be selected from the group consisting of indium, tin, zinc, nickel, gallium, carbon, and a combination thereof. The substrate can be selected from the group consisting of copper, tin, indium, iron, nickel, cobalt, gold, platinum, titanium, niobium, tantalum, molybdenum, tungsten, zinc, nickel, gallium, and a combination thereof.

An embodiment of the present disclosure provides for a device, among others, that includes: an anode; and a cathode, wherein the cathode includes a substrate having a material thereon. The material thereon can be selected from the group consisting of indium, tin, zinc, nickel, gallium, carbon, and a combination thereof. The substrate can be selected from the group consisting of copper, tin, indium, iron, nickel, cobalt, gold, platinum, titanium, niobium, tantalum, molybdenum, tungsten, zinc, gallium, carbon, and a combination thereof.

An embodiment of the present disclosure provides for a cathode, among others, that includes: a substrate having a material thereon. The material thereon can be selected from the group consisting of indium, tin, zinc, nickel, gallium, carbon, and a combination thereof. The substrate can be selected from the group consisting of copper, tin, indium, iron, nickel, cobalt, gold, platinum, titanium, niobium, tantalum, molybdenum, tungsten, zinc, gallium, carbon, and a combination thereof.

In any one or more aspects of any one or more of the embodiments, the material can include indium and the substrate can include indium, and formation of formic acid can be preferentially formed relative to CO and H_2. The material can include indium and the substrate can include copper, and formation of CO can be preferentially formed relative to formic acid and H_2. The substrate can be oxidized. The material can be a nanoparticle or a microparticle or both.

Other methods, devices, features, and advantages of the present disclosure will be or become apparent to one with skill in the art upon examination of the following drawings and detailed description. It is intended that all such additional systems, methods, features, and advantages be included within this description, be within the scope of the present disclosure, and be protected by the accompanying claims.

BRIEF DESCRIPTION OF THE DRAWINGS

Many aspects of the present disclosure can be better understood with reference to the following drawings. The components in the drawings are not necessarily to scale, with emphasis instead being placed upon clearly illustrating the principles of the disclosure. Moreover, in the drawings, like reference numerals designate corresponding parts throughout the several views.

Fig. 1.1.A illustrates the comparison of the current density profiles for OD-Cu and Cu-In, chronoamperometric analyses as shown in Fig. 1.1B illustrates OD-Cu and Fig.

1.1.C illustrates Cu-In, and the long-term stability test for the Cu-In catalyst at −0.6 V vs. RHE in 0.1 M $KHCO_3/CO_2$. Fig 1.1D illustrates electrolysis with long controlled potentials in 0.1 M $KHCO_3/CO_2$ at −0.6 V vs. RHE.

Fig. 1.2A illustrates an SEM image, and Fig. 1.2B illustrates HR-TEM image of Cu-In with FFT images from the bulk and the surface (inset). Fig. 1.2C illustrates EDS element mapping of the selected area, showing In and Cu

Fig. 1.3A illustrates XRD profiles and Fig. 1.3B illustrates In 3d and Cu 2p XPS spectra of the Cu-In sample.

Fig. 1.4A illustrates the comparison of current density profiles for OD-Cu and Cu-Sn, and Fig. 1.4B chronoamperometric analysis for the Cu-Sn catalyst in 0.1 M $KHCO_3/CO_2$. The deposition of Sn on Cu-OD was carried out in a similar manner as In deposition, from Sn^{2+} containing solution passing -3.3 mA cm^{-2} for 90 min or 18 C cm^{-2}.

Fig. 2.1A illustrates the chronoamperometric electrolysis profiles and Fig. 2.1B illustrates their Faradaic efficiencies using the CuIn electrode in CO_2-saturated 0.1 M $KHCO_3$ aq.

Fig. 2.2A illustrates the XRD profiles and Fig. 2.2B illustrates SEM images of the as-prepared and after-electrolysis CuIn electrodes.

Fig. 2.3A-B illustrate XPS spectra of (Fig. 2.3A) Cu 2p and (Fig. 2.3B) In 3d for as-prepared and after-electrolysis CuIn samples.

DISCUSSION

This disclosure is not limited to particular embodiments described, and as such may, of course, vary. The terminology used herein serves the purpose of describing particular embodiments only, and is not intended to be limiting, since the scope of the present disclosure will be limited only by the appended claims.

Where a range of values is provided, each intervening value, to the tenth of the unit of the lower limit unless the context clearly dictates otherwise, between the upper and lower limit of that range and any other stated or intervening value in that stated range, is encompassed within the disclosure. The upper and lower limits of these smaller ranges may independently be included in the smaller ranges and are also encompassed within the disclosure, subject to any specifically excluded limit in the stated range. Where the stated range includes one or both of the limits, ranges excluding either or both of those included limits are also included in the disclosure.

Embodiments of the present disclosure will employ, unless otherwise indicated, techniques of material science, chemistry, and the like, which are within the skill of the art. Such techniques are explained fully in the literature.

The following examples are put forth so as to provide those of ordinary skill in the art with a complete disclosure and description of how to perform the methods and use the compositions and compounds disclosed and claimed herein. Efforts have been made to ensure accuracy with respect to numbers (*e.g.*, amounts, temperature, *etc.*), but some errors and deviations should be accounted for. Unless indicated otherwise, parts are parts by weight, temperature is in °C, and pressure is at or near atmospheric. Standard temperature and pressure are defined as 20 °C and 1 atmosphere.

Before the embodiments of the present disclosure are described in detail, it is to be understood that, unless otherwise indicated, the present disclosure is not limited to particular materials, reagents, reaction materials, manufacturing processes, dimensions, frequency ranges, applications, or the like, as such can vary. It is also to be understood that the terminology used herein is for purposes of describing particular embodiments only, and is not intended to be limiting. It is also possible in the present disclosure that steps can be executed in different sequence, where this is logically possible. It is also possible that the embodiments of the present disclosure can be applied to additional embodiments involving measurements beyond the examples described herein, which are not intended to be limiting. It is furthermore possible that the embodiments of the present disclosure can be combined or integrated with other measurement techniques beyond the examples described herein, which are not intended to be limiting.

It should be noted that, as used in the specification and the appended claims, the singular forms "a," "an," and "the" include plural referents unless the context clearly dictates otherwise. Thus, for example, reference to "a support" includes a plurality of supports. In this specification and in the claims that follow, reference will be made to a number of terms that shall be defined to have the following meanings unless a contrary intention is apparent.

Discussion:

Embodiments of the present disclosure provide for converting CO_2 to CO and formic acid, electrodes, devices including electrodes, methods of making electrodes, and the like. Embodiments of the present disclosure are advantageous in that they can provide for

improved efficiencies for forming formic acid and/or CO in reducing CO_2 in the presence of water. In this regard, embodiments can provide for improved CO_2 reduction efficiency as compared to hydrogen evolution efficiency. In other words, embodiments can provide superior selectivity of CO_2 reduction products over the proton reduction product (H_2). In addition, the cathode can have an increased surface area, which improves current density profiles. Additional details are provided in the Example(s).

As noted above, an embodiment of the present disclosure provides for a method for converting CO_2 to CO and formic acid. In an embodiment, an electrochemical or photoelectrochemical cell, system, or device can be used to react CO_2 (*e.g.*, provided (*e.g.* bubbling) to the system or cell using a gas handling system) and H_2O (*e.g.*, under negatively applied potentials) to produce CO and formic acid. The reaction can take place at ambient temperature and pressure but can also be conducted at higher or lower temperatures and/or pressures.

In an embodiment, a cathode can be used that includes a substrate having a material thereon. In an embodiment, the substrate can be copper, tin, indium, iron, nickel, cobalt, gold, platinum, titanium, niobium, tantalum, molybdenum, tungsten, zinc, gallium, and carbon, and alloys, and oxidized forms thereof. The material can be disposed on about 5 to 75 % of the surface of the substrate. In an embodiment, the material can be disposed on the substrate using a technique such as electrodeposition, electrophoretic deposition, and drop-casting.

In an embodiment, the material can be one that has a high hydrogen overpotential (*e.g.*, about 500 mV, at 25 °C, 1 atm). In an embodiment, the material can be a metal, metal alloy, metal oxide, or a metal hydroxide. In an embodiment, the material can be indium, tin, zinc, gallium, nickel and carbon and a combination thereof, or alloys, oxides, mixed oxides, or hydroxides thereof. In an embodiment, the alloy can include Cu-In alloys. In an embodiment, the material can be in the form of a sheet or foil disposed on the substrate. In another embodiment, the material can include particles of the material such as microparticles, nanoparticles, or a mixture thereof.

In an embodiment, the alloy can be formed by the electrochemical deposition of one metal onto another, for example, indium (In) on copper (Cu), to make Cu-In alloy catalyst, as shown in Example 2. In another embodiment, the alloy can be formed from a mixed oxide to form the alloy, for example $CuInO_2$, can be reduced to Cu-In alloy, as shown in Example 1.

In an embodiment, when the material is indium and the substrate is indium, formation of formic acid is preferred selectively over the formation of CO and H_2. In an embodiment, when the material is indium and the substrate is copper, formation of CO is preferred over the formation of formic acid and H_2. Consequently, one can design the cathode for CO_2 reduction to generate a desired product(s). See the Examples for more details.

In an embodiment, other products can be produced such as methanol, methane, and higher hydrocarbons by changing the reactants and/or conditions. For example, methane can be generated by using Cu nanoparticles supported on glassy carbon as a cathode in 0.1 M $NaHCO_3$. Ethanol, methanol and higher hydrocarbons can be produced by further reduction of CO, which is the sole product in our system.

In general, electrochemical and photoelectrochemical cells are known. An exemplary embodiment of the present disclosure includes a glass electrolysis cell comprising of two chambers separated by a ceramic frit or ionic membrane, where the cell includes the cathode provided herein, an anode, an electrolyte, a reference electrode, and a gas inlet/outlet for gas sample analyzer. The anode can include an anode that is appropriate for the desired application. In an embodiment the anode can include nickel based anodes, cobalt based anodes, and iron based anodes. In an embodiment, the electrolyte can be an aqueous medium containing an acidic electrolyte (*e.g.*, citric acid, perchloric acid, hydroiodic acid, nitric acid, sulfuric acid, bromic acid, etc.) or basic electrolyte (*e.g.*, hydroxides, sodium amide, sodium hydride, etc.), simple salts, KCl, NaCl, $KHCO_3$, and $NaHCO_3$, and non-aqueous electrolytes which may comprise nBu_4NPF_6 (TBHP) in MeCN solution, and a combination thereof. In an embodiment the simple salts can include an anion (*e.g.*, chloride, fluoride, sulfate, nitrate, nitrite, phosphate, acetate, etc.) and a cation (*e.g.*, sodium, potassium, magnesium, iron, calcium, ammonium, etc.) such as $KHCO_3$, NaCl, KCl, LiCl, $CaCl_2$, or Na_2SO_4. The electrolytes may be employed at various pH levels depending upon the system, reactants, and products to be generated.

EXAMPLES

Example 1

The challenge in the electrochemical reduction of aqueous carbon dioxide is in designing a highly selective, energy efficient, and non-precious metal electrocatalyst that minimizes the competitive reduction of proton to form hydrogen during aqueous CO_2

conversion. Herein, a non-noble metal electrocatalyst based on a copper-indium (Cu-In) alloy that selectively converts CO_2 to CO with a low overpotential is reported.

The development of an artificial photosynthesis process that converts CO_2 and stores the energy in the form of chemical bonds is one of the grand challenges in modern chemistry.[1,2] However, the limited choice of electrocatalysts that are energy efficient, selective, and stable increases the complexity of this process.[3] Conventionally, metal electrodes have been utilized as electrocatalysts for the aqueous CO_2 reduction reaction, and the product distribution strongly depends on the nature of the electrode surface and the electrolyte.[3] Hori and coworkers observed that the CO_2 reduction reaction reproducibly yields CO, CH_4, HCOOH and other hydrocarbon products and that the selectivity of the products is determined by the nature of the metallic electrode.[3,4] Among the various metallic electrodes, copper has attracted special attentions because it is a metal that produces hydrocarbons during the CO_2 reduction reaction.[3-13]

Designing a CO_2-reducing electrocatalyst should thus be focused on the use of non-noble-metals that are selective and energy efficient. Recently, various strategies have been reported for the conversion of CO_2 including alloying of copper with other metals to obtain higher selectivity and energy efficiency.[14-21] The general trend is that the binding strengths of the intermediates on the catalyst surface need to be adequate and thus the importance of the surface coordinately unstaturated sites has been addressed.[6,9,11,22,23] This study focused on an indium electrodeposited Cu electrocatalyst, which resulted in the formation of a Cu-In alloy that works at moderate overpotentials with exclusive selectivity for CO and excellent stability.

Experimental protocol

To fabricate thick films of the Cu-In intermetallic, oxide-derived (OD-)Cu electrodes were first prepared. For this purpose, Cu foils (200 μm in thickness, 99.99%, Sigma-Aldrich) were cut to the desired electrode size (1×3 cm) and cleaned for several seconds in 1 M HCl. The electrodes were rinsed with Milli-Q water (18.2 MΩ cm @ 25 °C) and dried under ambient conditions. To acquire a smooth and uniform electrode surface, the electrodes were dried with Kimwipes soon after rinsing to avoid any partial oxidation of the electrodes from air. The cleaned electrodes were placed vertically in a ceramic crucible and thermally oxidized at 773 K for 2 h under static air in a muffle furnace. Thereafter, the Cu-In electrode was prepared through the in situ electrochemical reduction of the thermally

oxidized Cu electrodes in 0.05 M $In_2(SO_4)_3$/0.4 M citric acid at a current density of −10 mA for 90 min (~18 C cm^{-2}).

Scanning Electron Microscopy (SEM) was conducted using a NovaNano SEM from FEI Instruments. X-ray diffraction (XRD) patterns were recorded on a Bruker D8 Advanced A25 diffractometer equipped with a Cu X-ray tube (Cu–K_α; $\lambda = 0.154$ nm) operated at 40 kV and 40 mA. XPS studies were conducted using an AMICUS/ESCA 3400 KRATOS equipped with a Mg-anode Kα excitation X-ray source ($h\nu$ = 1253.6 eV) operated at 10 kV and 10 mA. During the experiments, the pressure in the analysis chamber was maintained at ~2×10^{-6} Pa. The measured binding energies were calibrated based on the C 1s binding energy at 284.8 eV. The samples were analyzed using transmission electron microscopy (TEM) to study the morphology, crystal structure, and the elemental distributions of Cu and In in the Cu-In crystals. TEM analysis of the samples was performed using a TitanG2 80-300 CT from FEI Instruments that was equipped with a field-emission-gun and a GIF Tridiem863 energy-filter from Gatan, Inc. Moreover, the analysis was conducted by the operating the microscope with a beam energy of 300 keV. Note that the TEM specimens were prepared by placing a small amount of samples on holey carbon-coated nickel (Ni) grids with a mesh size of 300. Several low- and high-resolution electron micrographs were acquired from various locations during the analysis. Fast-Fourier transform (FFT) analysis was applied to various regions of the High-resolution TEM (HRTEM) micrographs to investigate the different crystal structures within the Cu-In crystals. In addition, selected-area electron diffraction (SAED) and X-ray energy dispersive spectroscopy (EDS) were also performed to investigate the crystal structures and elemental compositions of the samples. The Cu and In maps were acquired by setting the GIF filter to imaging mode. Note that the Cu-L23 (2p-3d) and In-M45 (3d-4f) electron energy-loss spectroscopy (EELS) edges were selected to create the Cu and In elemental maps, respectively. Moreover, the so-called 3-window method was employed to generate the maps.

A custom-made electrochemical cell was employed, and a BioLogic© VMP3 potentiostat was utilized. Three electrodes were used to monitor the current-potential response of the working electrode. A Pt wire and an Ag/AgCl electrode (in saturated KCl) were employed as a counter electrode and as a reference electrode, respectively. The counter electrode was isolated with a ceramic frit, so that the product crossover was effectively suppressed. For the electrochemical reduction of CO_2, 0.1 M $KHCO_3$ (99.99%, metal basis, Sigma-Aldrich) was used as an electrolyte for the CO_2 conversion studies. Prior

to the measurements, the electrolyte was saturated with CO_2 for 1 h. A continuous flow of CO_2 was maintained during the electrolysis, providing large current densities for the CO_2 reduction products to minimize the mass transport limitations. A flow rate of 10 ml min^{-1} was used to ensure sufficient CO_2 transport to the electrode surface while preventing interference from gas bubbles striking the electrode. All of the applied potentials were recorded against a Ag/AgCl (saturated KCl) reference electrode and then converted to Reversible Hydrogen Electrode (RHE) using E (vs. RHE) = E (vs. Ag/AgCl) + 0.197 V + 0.0591 V*pH.

To confirm the identities and quantities of the liquid and gas phase products during the electrochemical reactions, an offline High Performance Liquid Chromatograph (HPLC, Agilent 1200 series) and an online micro gas chromatograph (SRI instruments, T-3000) were employed, respectively. For analysis of the gaseous products, a packed MolSieve 5A was used, which was equipped with a thermal conductivity detector (TCD). To quantify the liquid products, the HPLC was equipped with an ICE-Coregel 87 H3 column. The minimum detection limit for gaseous products was 50 ppm. Induction period of 0.3 h for gas analyses is observed due to filling dead-space of the reactor to the inlet of GC.

Results and discussion

Oxide-derived (OD)-Cu substrate was obtained by thermally oxidizing a Cu metal sheet at 773 K for 2 h in static air.[13] This treatment led to the formation of a hairy CuO nanowire structure on Cu_2O-Cu layers,[13] resulting in a surface roughness factor that was increased 140-fold compared to that of the pristine Cu sheet as measured by cyclic voltammetry. The Cu-In electrode was then prepared through electrochemical reduction of the OD-Cu in 2-electrode system with a solution containing 0.05 M $InSO_4$ and 0.4 M citric acid at a current density of −3.3 mA cm^{-2} for 90 min (~18 C cm^{-2}). This deposition of In underwent a rather complex reduction process, in which both reduction of the Cu oxide and deposition of In occurred. The surface roughness was further improved to double of OD-Cu.

The Cu-In electrode was subsequently tested at different applied potentials and compared with OD-Cu. **Figs. 1.1A-D** show the total current density (j_{tot}) and FE at −0.3 to −0.7 V vs. RHE in 0.1 M $KHCO_3/CO_2$. As shown in **Fig. 1.1A**, similar values for total current density, j_{tot}, were obtained for OD-Cu and Cu-In in the same potential range and electrochemical conditions. These results indicate that the electron transfer rates are essentially identical in these electrodes; however, they exhibited a distinct difference in

selectivity. The effects of the applied potentials on the FEs for OD-Cu and Cu-In are shown in **Figs. 1.1B and 1.1C**, respectively. OD-Cu began to convert CO_2 at a potential of −0.3 V vs. RHE, primarily generating H_2 as the reaction product. When the electrode was more negatively polarized, the conversion of CO_2 to CO and HCOOH improved, reaching maximum FE of 40 and 30 %, respectively, at −0.6 V vs. RHE, consistent with the literature.[7,13] In contrast, the Cu-In electrode catalyzed the reduction of CO_2 at 0.3 V vs. RHE, to CO selectively (FE_{CO} ~ 23%) while suppressing the formation of H_2 (FE_{H2} ~ 3%). We were unable to capture the remaining products, probably because of additional Cu and/or In reduction as the Cu/Cu^{x+} or In/In^{y+} standard redox potentials reside in this range.[28] Moreover, at applied potentials from −0.3 to −0.7 V vs. RHE, CO was produced as almost the sole product of CO_2 reduction, approaching an FE of 90% at −0.5 V vs. RHE. It is clear that the presence of In along with Cu drastically altered the nature of the electroactive species.

To evaluate the stability of the Cu-In catalyst, electrolysis with long controlled potentials in 0.1 M $KHCO_3/CO_2$ at −0.6 V vs. RHE was performed, as shown in **Fig. 1.1D**. The reaction was intentionally stopped after 3.5 h and allowed to stand overnight to observe the degradation of the electrode under open-circuit aqueous conditions. The reaction was then restarted for an additional 3.5 h. The results indicated that the Cu-In catalyst is extremely stable under the conditions for aqueous CO_2 reduction, with an 85% FE for CO for 7 h.

Fig. 1.2A presents SEM image of the Cu-In structure. The microstructure consists of large irregularly shaped grains ranging from 100 to 500 nm in size. The large grains are formed as a result of the agglomeration of small nanoparticles (~50 nm), which are capped by a shell-like structure. High-resolution transmission electron micrographs (HR-TEM) and the corresponding calculated fast Fourier transform (FFT) patterns of the Cu-In samples after the CO_2 reduction experiments are shown in **Fig. 1.2B**. The nanostructure could be divided into two distinct regions: the bulk and the surface. The FFT pattern of the core clearly shows a highly crystalline structure, whereas the FFT pattern of the shell shows a deformed crystal structure, which may arise from the diffusion of In, with a large atomic radius (0.155 nm), into the smaller Cu (0.135 nm) lattice. Superimposed elemental maps of In and Cu are shown in **Fig. 1.2C**. The In appears primarely in a thin line about the periphery (surface) of the structure and as specs interspersed within the structure. The figure clearly shows that the surface is enriched with In with a thickness of ~3 nm. The XRD

pattern of the Cu-In sample (**Fig. 1.3A**) confirms the formation of the Cu-In bimetallic ($Cu_{11}In_9$) alloy (PDF#00-065-4963), with intense peaks for the Cu metal substrate (PDF#00-004-0836). The X-ray photoelectron spectra for Cu $2p_{3/2}$ and Cu $2p_{1/2}$ and for In $3d_{5/2}$ and $3d_{3/2}$ (**Fig. 1.3B**) indicate the reduction to the Cu^0 and In^0 metallic states. Overall, the characterization suggests that the thin layer of bimetallic Cu-In alloy was uniformly formed on the rough surface of OD-Cu.

The experimental data presented here raise a very important question regarding the influence of the environment on the nature of the active species when a second metal center is present along with Cu. A separate CO_2 reduction experiment with an In-deposited Cu sheet without an initial oxidation treatment showed only slight improvement in CO selectivity (H_2 predominant), indicating that having OD-Cu as the starting substrate is effective. This result may indicate that the high surface area with grain boundaries,[7] and the specific surface facets created by the oxidation/re-reduction treatment are essential for achieving high selectivity toward CO at low overpotentials. Another experiment with an In-deposited In sheet resulted in formic acid as the major product with trace amounts of H_2 at elevated overpotentials (typically < -0.9 V vs. RHE), indicating that In alone will not lead to the formation of CO and Cu is essential. Furthermore, a similar increase in selectivity towards CO was observed using Sn as the second metal (**Figs. 1.4A-B**), suggesting that the universal effects of the second metals that have high overpotentials toward the evolution of H_2 prevail. When a high hydrogen overpotential metal such as In is present around the Cu active site, effectively forming a Cu-In alloy, it presumably inhibits the formation of H_2 on Cu without deactivating the reduction of CO_2.

In summary, our results show that a Cu-In sample prepared via the in situ reduction of Cu_2O in an $InSO_4$ solution selectively catalyzed the reduction of CO_2 to CO with a high FE and with extremely high stability for the electrocatalysis. Moreover, these catalysts suppress the reduction of H^+ and simultaneously promote the conversion of CO_2, which is highly desired in the electrochemical recycling of aqueous CO_2. Additionally, Cu-In electrodes are composed of non-precious metals and can be readily prepared and scaled up for commercial applications. Naturally, this material can also be applied for CO electrochemical conversion.[16] Thus, we believe that Cu-In catalyst is the first step toward obtaining efficient, selective and low-cost electrocatalysts in the future.

Reference

1. T. A. Faunce, W. Lubitz, A. W. Rutherford, D. MacFarlane, G. F. Moore, P. Yang, D. G. Nocera, T. A. Moore, D. H. Gregory, S. Fukuzumi, K. B. Yoon, F. A. Armstrong, M. R. Wasielewski and S. Styring, *Energy Environ. Sci.*, 2013, **6**, 695-698.

2. N. S. Lewis and D. G. Nocera, *Proc. Natl. Acad. Sci.*, 2006, **103**, 15729-15735.

3. K. J. P. Schouten, F. Calle-Vallejo and M. T. M. Koper, *Angew. Chem. Int. Ed.*, 2014, **53**, 10858-10860.

4. Y. Hori, in *Modern aspects of electrochemistry*, ed. C. Vayenas, Springer, New York, 2008.

5. Y. Hori, H. Wakebe, T. Tsukamoto and O. Koga, *Electrochim. Acta*, 1994, **39**, 1833-1839.

6. E. E. Barton, D. M. Rampulla and A. B. Bocarsly, *J. Am. Chem. Soc.*, 2008, **130**, 6342-6344.

7. K. P. Kuhl, E. R. Cave, D. N. Abram and T. F. Jaramillo, *Energy Environ. Sci.*, 2012, **5**, 7050-7059.

8. Y. Yan, E. L. Zeitler, J. Gu, Y. Hu and A. B. Bocarsly, *J. Am. Chem. Soc.*, 2013, **135**, 14020-14023.

9. J. L. DiMeglio and J. Rosenthal, *J. Am. Chem. Soc.*, 2013, **135**, 8798-8801.

10. B. A. Rosen, A. Salehi-Khojin, M. R. Thorson, W. Zhu, D. T. Whipple, P. J. A. Kenis and R. I. Masel, *Science*, 2011, **334**, 643-644.

11. C. Costentin, M. Robert and J.-M. Saveant, *Chem. Soc. Rev.*, 2013, **42**, 2423-2436.

12. H. A. Hansen, J. B. Varley, A. A. Peterson and J. K. Nørskov, *J. Phys. Chem. Lett.*, 2013, **4**, 388-392.

13. H.-K. Lim, H. Shin, W. A. Goddard, Y. J. Hwang, B. K. Min and H. Kim, *J. Am. Chem. Soc.*, 2014, **136**, 11355-11361.

14. A. T. Garcia-Esparza, K. Limkrailassiri, F. Leroy, S. Rasul, W. Yu, L. Lin and K. Takanabe, *J. Mater. Chem. A*, 2014, **2**, 7389-7401.

15. C. W. Li, J. Ciston and M. W. Kanan, *Nature*, 2014, **508**, 504-507.

16. K. P. Kuhl, T. Hatsukade, E. R. Cave, D. N. Abram, J. Kibsgaard and T. F. Jaramillo, *J. Am. Chem. Soc.*, 2014, **136**, 14107-14113.

17. W. Zhu, R. Michalsky, Ö. Metin, H. Lv, S. Guo, C. J. Wright, X. Sun, A. A. Peterson and S. Sun, *J. Am. Chem. Soc.*, 2013, **135**, 16833-16836.

18. Q. Lu, J. Rosen, Y. Zhou, G. S. Hutchings, Y. C. Kimmel, J. G. Chen and F. Jiao,

Nat. Commun., 2014, **5**.

19. X. Nie, M. R. Esopi, M. J. Janik and A. Asthagiri, *Angew. Chem. Int. Ed.*, 2013, **52**, 2459-2462.

20. R. Reske, H. Mistry, F. Behafarid, B. Roldan Cuenya and P. Strasser, *J. Am. Chem. Soc.*, 2014, **136**, 6978-6986.

21. W. Tang, A. A. Peterson, A. S. Varela, Z. P. Jovanov, L. Bech, W. J. Durand, S. Dahl, J. K. Norskov and I. Chorkendorff, *Phys. Chem. Chem. Phys.*, 2012, **14**, 76-81.

22. A. A. Peterson and J. K. Nørskov, *J. Phys. Chem. Lett.*, 2012, **3**, 251-258.

23. J. Christophe, T. Doneux and C. Buess-Herman, *Electrocatal.*, 2012, **3**, 139-146.

Example 2

The lack of availability of efficient, selective and stable electrocatalysts is a major hindrance for scalable CO_2 reduction processes. Herein, we report the generation of Cu-In alloy surfaces for electrochemical reduction of CO_2 from mixed metal oxides of $CuInO_2$ as the starting material. The material successfully generates the selective active sites to form CO from CO_2 electroreduction at mild overpotentials. This study demonstrates an example of a scalable synthesis method of bimetallic surfaces utilized with the mixed oxide precursor having the diversity of metal choice, which may drastically alter the electrocatalytic performance, as presented herein.

The construction of the electrocatalysts that can efficiently activate stable CO_2 molecules has proven to be a significant challenge. The challenge is made more serious when attempting to control selectivity, as the process generates several different products because of the complex multiple electron and proton coupling steps required to yield hydrocarbons. Hori et al. performed pioneering works on electrochemical CO_2 reduction, where most of the transition metal electrocatalysts were studied.[1,2] In addition to metals, also semiconductors, oxide-derived metallic electrodes, and alloys have been investigated as electrocatalysts in order to identify well performing electrodes.[3] However, due to inefficiency, low selectivity, instability, and the high costs of most of the catalysts investigated for the CO_2 reduction to date, new avenues for electrocatalyst design are required.

Numerous strategies have previously been devised to control the reaction chemistry of the CO_2 reduction utilizing one-electron shuttle,[4] ionic liquids,[5,6] organic compounds and organometallic complexes.[7] More recently, two different

approaches, bimetallic[8-11] and oxide-derived metal electrodes,[12-14] have received much attention. In both approaches, much focus has been given to tuning the binding strengths of the intermediates on the surface of the catalyst to improve the reaction kinetics of the CO_2 reduction.

In general, the CO_2 reduction activity and the product selectivity depend on the nature of the electrolyte, temperature, pressure, the stabilization of the $CO_2^{\bullet-}$ radical,[1] and, most importantly, on the binding energy of CO,[15] which is a fundamental intermediate in the reduction of CO_2, to the surface of the catalyst employed. For example, Pt group metals initially reduce CO_2 to produce CO, which binds strongly to the surface, poisoning the electrode, preventing further CO_2 reactivity, and hydrogen (H_2) is generated as the main product from the competing reduction of water.[1] In contrast, Au[16] and Ag[17] bind CO weakly to release CO from the surface before further electron-proton coupled transfer occurs to generate hydrocarbons. Cu possesses an intermediate binding energy for CO, which provides not only successive electron/proton transfers but also offers the potential for C-C coupling as well to produce methane (CH_4), methanol (CH_3OH) or ethanol (C_2H_5OH).[8,11,18-20]

To further tune the reactivity of Cu catalysts, the incorporation of heteroatoms on the surface is considered to affect the reactivity towards CO_2 activation.[21] Synergistic effects caused by the heteroatoms lead to both electronic and geometric alteration of the active sites, which may in turn cause drastic changes in the activity and selectivity for CO_2 conversion.

In this Example, we designed a unique generation of CuIn alloy active sites, starting from $CuInO_2$. The two metal atoms in the mixed oxide precursors were essentially dispersed in an alternating manner in their crystal structures at the atomic scale, so that reduction of such oxides is expected to generate well mixed alloy active sites. The bimetallic approach would alter the local electronic and geometric environment, resulting in better control over selectivity. As a result, the identity of heteroatoms rather surprisingly alters the performance of the CO_2 catalysis.

Experimental protocol

For the synthesis of $CuInO_2$, first, In_2O_3 (Aldrich 99.9%) was mixed with Na_2CO_3 (Aldrich 99.999%) in a 1:1 molar ratio and then heated at 1273 K to prepare

$NaInO_2$ in a tube furnace (Nabertherm RS 80/300/13, tube I.D. 70 mm) under a high flow of nitrogen gas (1.5 L min^{-1}). Next, the $NaInO_2$ was reacted with CuCl in a 1:1 molar ratio and then heat treated at 673 K for 12 h under flowing N_2.[22] For reference, Cu_2O (Aldrich ≥99.99%) was used as purchased.

For the electrochemical investigation, a custom-made three-electrode system was employed, controlled by a BioLogic© VMP3 potentiostat. Pt wire and Ag/AgCl (in saturated KCl) were used as the counter and reference electrodes, respectively. All the applied potentials are reported as reversible hydrogen electrode (RHE) potentials, which were measured through accurate measurements of the pH. The working electrode from the powder $CuInO_2$ was fabricated using the electrophoretic deposition method.[23] The geometric area used was typically 1.5 × 2 cm^2 carbon paper (Toray TGP-H-60) for both working and counter electrodes. During electrophoretic deposition, colloidal particles of each electrocatalyst (~ 0.5 g) were suspended using ultrasonication in reagent-grade acetone (50 ml) with a small amount of iodine (~ 50 mg). Homogenous films on carbon paper were obtained under an applied potential of 30 V for 3 min. The films were dried at 373 K in vacuum for 12 h. The control experiment shows that the currents originated from the bare carbon paper electrode were negligible at the relevant potential range reported hereafter.

For CO_2 conversion studies, the as-prepared Cu oxide electrodes were first subjected to the CO_2 reduction conditions in 0.1 M $KHCO_3$ (99.99%, metal basis, Sigma-Aldrich) under chronopotentiometric conditions at −1.67 mA cm^{-2} to obtain reduced electrodes. The $KHCO_3$ electrolyte was saturated with a continuous flow of CO_2 (10 ml min^{-1}), and the final pH was 6.8. Further experiments at different potentials were performed using the obtained reduced electrodes.

To quantify the gas- and liquid-phase products for the CO_2 reduction experiments, an on-line gas analyzer (H_2, CO, CH_4, CO_2, C_2H_6, C_2H_4), an off-line gas chromatograph with a flame ionization detector (CH_3OH), and a high-performance liquid chromatography instrument (HPLC, Agilent 1200 series) (HCOOH, CH_3COOH and other oxygenates) were employed. The on-line microGC (SRI Instruments, T-3000) was equipped with the following two channels: 1) 5A molecular sieves and a thermal conductivity detector using Ar as a carrier gas, and 2) HayeSep Q and a thermal conductivity detector. The minimum detection limit for the gas products was 50 ppm.

Powder X-ray diffraction (XRD) patterns in the 2θ range of 10–80° were recorded to investigate the crystalline nature and phase purity of the products. The XRD patterns of the powder samples were recorded on a Bruker model D8 Advance. Cu-Kα radiation from a Cu anode X-ray tube operated at 40 kV and 40 mA was used as an X-ray source for collecting the XRD patterns. X-ray photoelectron spectroscopy (XPS) was conducted using an AMICUS system (Kratos Analytical). All the peaks were calibrated on the basis of the C 1s peak at 284.8 eV.

Results and discussion

Electrocatalytic performance and characterization of Cu-In catalyst

The bimetallic $CuInO_2$ derived electrode was tested at various applied potentials. **Fig. 2.1A** shows the total current density (j_{tot}) and FE at different potentials from −0.4 to −0.8 V vs. RHE in 0.1 M $KHCO_3/CO_2$ for 1 h. **Fig. 2.1A** shows that the overall current density of the electrode increases with the applied potential, and a steady-state current was obtained at each potential when tested for at least 1 h. Although the chronoamperometric measurement at various potentials was conducted using the identical electrode, the stable currents were measured at each potential (for more than 5 h), demonstrating the excellent stability of the electrode. The product selectivities at different potentials are shown in **Fig. 2.1B**. The product distribution at a given potential remained almost unchanged during our measurement, consistent with the highly stable nature of the electrode. The CuIn electrode starts to convert CO_2 at approximately −0.4 V vs. RHE, generating CO with an FE of 11% while cogenerating H_2 as a main product (FE 45%). We could not capture the remaining products by HPLC and GC, probably associated with undesired metal redox reactions. When the CuIn electrode was further negatively polarized, the selectivity of the CO_2 reduction product was enhanced at applied potentials from −0.5 to −0.8 V vs. RHE. The FE for the CO_2 reduction products at −0.8 V vs. RHE reached ~ 90% (FEs of CO and HCOOH are 70 and 19%, respectively), whereas the H_2 selectivity was under 10%. This selectivity effect was prominent only when both In and Cu were present, as Cu or In alone produced mostly H_2 or HCOOH, respectively. The improved Faradaic efficiency for CO_2 reduction using CuIn surfaces is likely due to different local geometric and electronic environments around the Cu sites.

Figs. 2.2A-B show the XRD profile and SEM image of the as-prepared and after-electrolysis CuIn sample. The XRD pattern of the as-prepared sample in **Fig. 2.2A** shows the major pattern ascribable to $CuInO_2$, along with the $NaInO_2$ precursor and In_2O_3 as impurity phases. For the sample after the electrolysis, the major peaks assigned to metallic $Cu_{11}In_9$, Cu_7In_3 and Cu were observed, in addition to the peaks associated with the carbon substrate, consistent with the phase diagram of Cu-In system.[24] It was confirmed that the $CuInO_2$ phase was reduced to form the metallic phase. The SEM image of the as-prepared sample in **Fig. 2.2B** shows large particle aggregates consisting of a macroporous structure. After electrolysis, some rough textures with some small porosity were observed as a result of the reduction of the solid bulk $CuInO_2$ particles (O removal), thereby shrinking the volume of crystal structures.

The surface states of the $CuInO_2$ and CuIn electrodes were investigated by XPS, as shown in **Figs. 2.3A-B**. In the case of the XPS spectra of the Cu 2p core level of $CuInO_2$, the broad Cu $2p_{3/2}$ and Cu $2p_{1/2}$ peaks at 934.8 and 954.6 eV were attributed to Cu(II) surface oxide. The Cu(II) oxide species exhibit satellite peaks at 942.3 and 944.9 eV because of the partially filled Cu $3d^9$ shells.[25] In the case of In, the peaks positioned at 445.1 and 452.8 eV could be assigned to In $3d_{5/2}$ and In $3d_{3/2}$, respectively.[26] Upon the reduction of $CuInO_2$, a shift towards lower binding energies in both the Cu 2p and In 3d peaks were observed, exhibiting the Cu^0 and In^0 states, consistent with the XRD profile (**Fig. 2.2A**).

Noticeably, the synthesis of mixed oxide powder precursors is easily scalable. Thus, we believe that multi-metallic functional catalysts can be further tailored to reduce CO_2 to obtain higher hydrocarbons, which is still a challenge in realizing efficient electrochemical CO_2 conversion. It is worth mentioning that the electrodeposition of In on flat Cu sheet improved only minimal Faradaic efficiency for CO_2 reduction.[10] The CuIn alloy originating from oxidized surfaces seems more effective, leaving the possibility that some unique facets generated from rough surfaces are specifically effective for CO_2 reduction (or H_2 evolution).

Conclusions

Mixed bimetallic $CuInO_2$ was successfully used as a precursor to generate CuIn alloy electrocatalysts for reduction of CO_2. The sample was found to

remarkably improve the selectivity of the CO_2 reduction to form CO and formic acid, with a total FE of 94% for CO_2 conversion. The CuIn electrode shows excellent stability under CO_2 reduction conditions, which is highly desired in the electrochemical recycling of CO_2. Structural characterization identified the CuIn alloy phase. The generation of bimetallic sites from mixed oxide reduction has diversity in the choice of metals; thus, the resultant selectivity for CO_2 electrocatalytic reduction can further be improved using this strategy.

References

1. Y. Hori, in *Modern aspects of electrochemistry*, ed. C. Vayenas, Springer, New York, 2008.

2. Y. Hori, H. Wakebe, T. Tsukamoto and O. Koga, *Electrochim. Acta*, 1994, **39**, 1833-1839.

3. E. E. Barton, D. M. Rampulla and A. B. Bocarsly, *J. Am. Chem. Soc.*, 2008, **130**, 6342-6344.

4. Y. Yan, E. L. Zeitler, J. Gu, Y. Hu and A. B. Bocarsly, *J. Am. Chem. Soc.*, 2013, **135**, 14020-14023.

5. J. L. DiMeglio and J. Rosenthal, *J. Am. Chem. Soc.*, 2013, **135**, 8798-8801.

6. B. A. Rosen, A. Salehi-Khojin, M. R. Thorson, W. Zhu, D. T. Whipple, P. J. A. Kenis and R. I. Masel, *Science*, 2011, **334**, 643-644.

7. C. Costentin, M. Robert and J.-M. Saveant, *Chem. Soc. Rev.*, 2013, **42**, 2423-2436.

8. J. Christophe, T. Doneux and C. Buess-Herman, *Electrocatal.*, 2012, **3**, 139-146.

9. D. Kim, J. Resasco, Y. Yu, A. M. Asiri and P. Yang, *Nat. Commun*, 2014, **5**.

10. S. Rasul, D. H. Anjum, A. Jedidi, Y. Minenkov, L. Cavallo and K. Takanabe, *Angew. Chem. Int. Ed.*, 2015, **54**, 2146-2150.

11. A. S. Varela, C. Schlaup, Z. P. Jovanov, P. Malacrida, S. Horch, I. E. L. Stephens and I. Chorkendorff, *J. Phys. Chem. C*, 2013, **117**, 20500-20508.

12. Y. Chen, C. W. Li and M. W. Kanan, *J. Am. Chem. Soc.*, 2012, **134**, 19969-19972.

13. A. T. Garcia-Esparza, K. Limkrailassiri, F. Leroy, S. Rasul, W. Yu, L. Lin and K. Takanabe, *J. Mater. Chem. A*, 2014, **2**, 7389-7401.

14. C. W. Li, J. Ciston and M. W. Kanan, *Nature*, 2014, **508**, 504-507.

16. K. P. Kuhl, T. Hatsukade, E. R. Cave, D. N. Abram, J. Kibsgaard and T. F. Jaramillo, *J. Am. Chem. Soc.*, 2014, **136**, 14107-14113.

17. W. Zhu, R. Michalsky, Ö. Metin, H. Lv, S. Guo, C. J. Wright, X. Sun, A. A. Peterson and S. Sun, *J. Am. Chem. Soc.*, 2013, **135**, 16833-16836.

18. X. Nie, M. R. Esopi, M. J. Janik and A. Asthagiri, *Angew. Chem. Int. Ed.*, 2013, **52**, 2459-2462.

19. R. Reske, H. Mistry, F. Behafarid, B. Roldan Cuenya and P. Strasser, *J. Am. Chem. Soc.*, 2014, **136**, 6978-6986.

20. W. Tang, A. A. Peterson, A. S. Varela, Z. P. Jovanov, L. Bech, W. J. Durand, S. Dahl, J. K. Norskov and I. Chorkendorff, *Phys. Chem. Chem. Phys.*, 2012, **14**, 76-81.

21. H.-K. Lim, H. Shin, W. A. Goddard, Y. J. Hwang, B. K. Min and H. Kim, *J. Am. Chem. Soc.*, 2014, **136**, 11355-11361.

22. Y. H. M. Shimode, M. Sasaki and K. Mukaida, *Mater. Trans. JIM* 2000, **41**, 1111-1113.

23. R. Abe, M. Higashi, K. Domen, *J. Am. Chem. Soc.*, 2010, **132**, 11828-11829.

24. L. Baqué, D. Torrado, G. Aurelio, D. G. Lamas, S. F. Aricó, A. F. Craievich and S. Sommadossi, *J. Phase Equilib. Diffus.*, 2014, **35**, 2-10.

25. S. Yamamoto, H. Bluhm, K. Andersson, G. Ketteler, H. Ogasawara, M. Salmeron and A. Nilsson, *J. Phys. Condens. Matter*, 2008, **20**, 184025.

26. R. W. Hewitt and N. Winograd, *J. Appl. Phys.*, 1980, **51**, 2620-2624.

It should be noted that ratios, concentrations, amounts, and other numerical data may be expressed herein in a range format. It is to be understood that such a range format is used for convenience and brevity, and thus, should be interpreted in a flexible manner to include not only the numerical values explicitly recited as the limits of the range, but also to include all the individual numerical values or sub-ranges encompassed within that range as if each numerical value and sub-range is explicitly recited. To illustrate, a concentration range of "about 0.1% to about 5%" should be interpreted to include not only the explicitly recited concentration of about 0.1 wt% to about 5 wt%, but also include individual concentrations (e.g., 1%, 2%, 3%, and 4%) and the sub-ranges (e.g., 0.5%, 1.1%, 2.2%, 3.3%, and 4.4%) within the indicated range. In an embodiment, the term "about" can

include traditional rounding according to the measuring technique and the numerical value. In addition, the phrase "about 'x' to 'y'" includes "about 'x' to about 'y'".

While only a few embodiments of the present disclosure have been shown and described herein, it will become apparent to those skilled in the art that various modifications and changes can be made in the present disclosure without departing from the spirit and scope of the present disclosure. All such modification and changes coming within the scope of the appended claims are intended to be carried out thereby.

CLAIMS

We claim at least the following:

1. A method of converting CO_2 to CO and formic acid, comprising:

exposing CO_2 and H_2O to a cathode to form formic acid and O_2 at an anode, wherein the cathode includes a substrate having a material thereon, wherein the material is selected from the group consisting of indium, tin, zinc, nickel, gallium, carbon, and a combination thereof, and wherein the substrate is selected from the group consisting of copper, tin, indium, iron, nickel, cobalt, gold, platinum, titanium, niobium, tantalum, molybdenum, tungsten, zinc, nickel, gallium, and a combination thereof.

2. The method of claim 1, wherein when the material includes indium and the substrate includes indium, formation of formic acid is preferentially formed relative to CO and H_2.

3. The method of claim 1 or 2, wherein when the material includes indium and the substrate includes copper, formation of CO is preferentially formed relative to formic acid and H_2.

4. The method of any of claims 1-3, wherein the substrate is oxidized.

5. The method of any of claims 1-4, wherein the material is a nanoparticle.

6. A device, comprising:

an anode; and

a cathode, wherein the cathode includes a substrate having a material thereon, wherein the material is selected from the group consisting of indium, tin, zinc, nickel, gallium, carbon, and a combination thereof, and wherein the substrate is selected from the group consisting of copper, tin, indium, iron, nickel, cobalt, gold, platinum, titanium, niobium, tantalum, molybdenum, tungsten, zinc, gallium, carbon, and a combination thereof.

7. The device of claim 6, wherein the material includes indium and the substrate includes indium.

8. The device of claim 6 or 7, wherein the material includes indium and the substrate includes copper.

9. The device of any of claims 6-8, wherein the substrate is oxidized.

10. The device of any of claims 6-9, wherein the material is a nanoparticle.

11. A cathode, comprising:

a substrate having a material thereon, wherein the material is selected from the group consisting of indium, tin, zinc, nickel, gallium, carbon, and a combination thereof, and wherein the substrate is selected from the group consisting of copper, tin, indium, iron, nickel, cobalt, gold, platinum, titanium, niobium, tantalum, molybdenum, tungsten, zinc, gallium, carbon, and a combination thereof.

12. The cathode of claim 11, wherein the material includes indium and the substrate includes indium.

13. The cathode of claim 11 or 12, wherein the material includes indium and the substrate includes copper.

14. The cathode of any of claims 11-13, wherein the substrate is oxidized.

15. The cathode of any of claims 11-14, wherein the material is a nanoparticle.

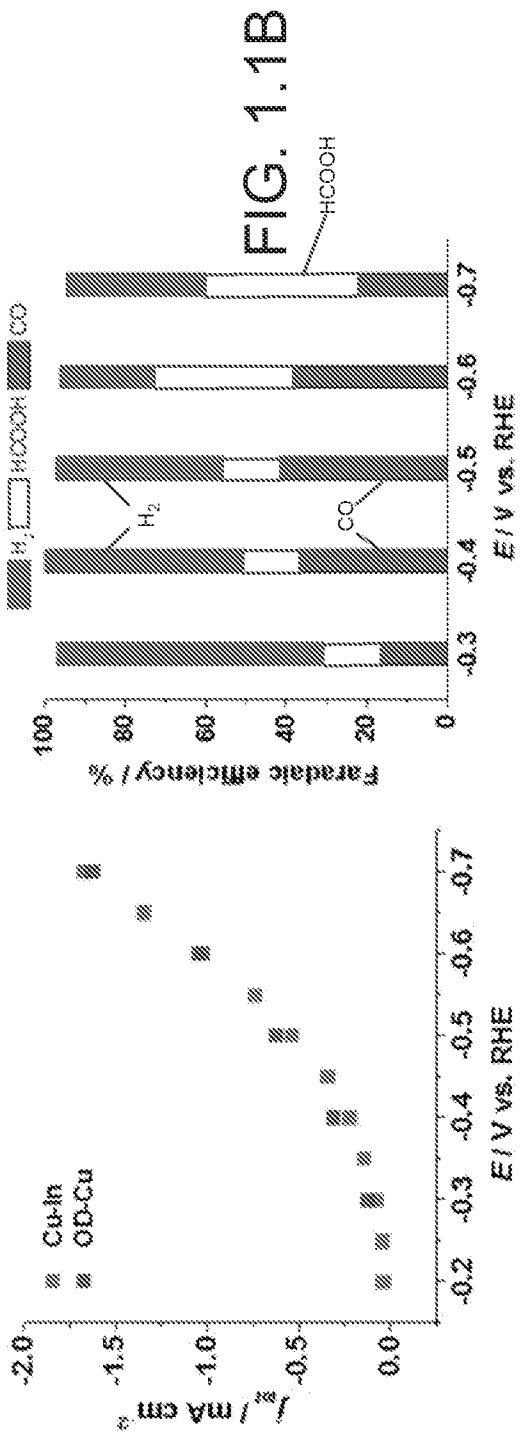

FIG. 1.1A

FIG. 1.1B

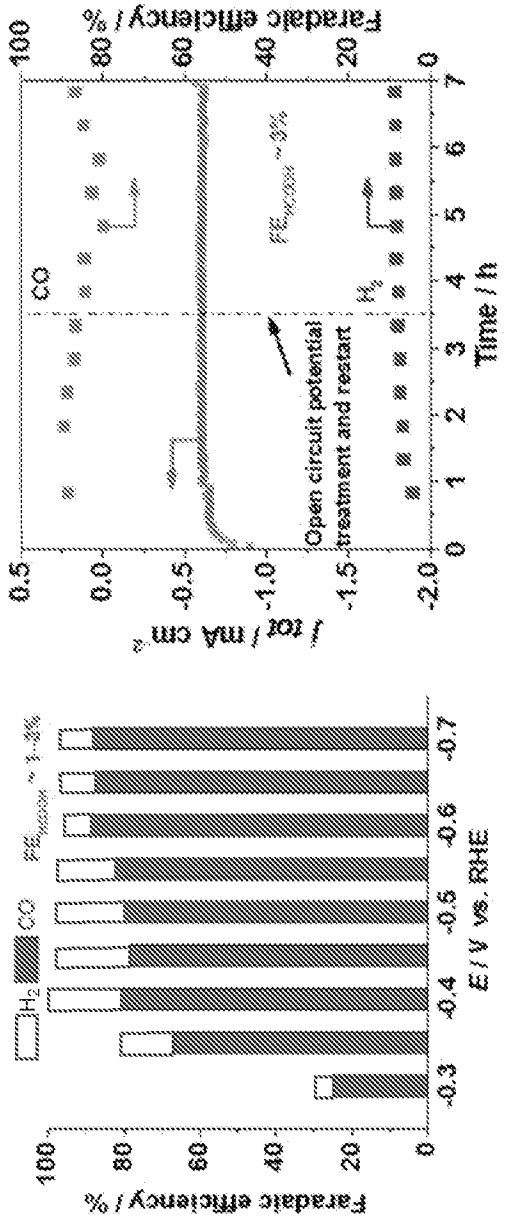

FIG. 1.1D

FIG. 1.1C

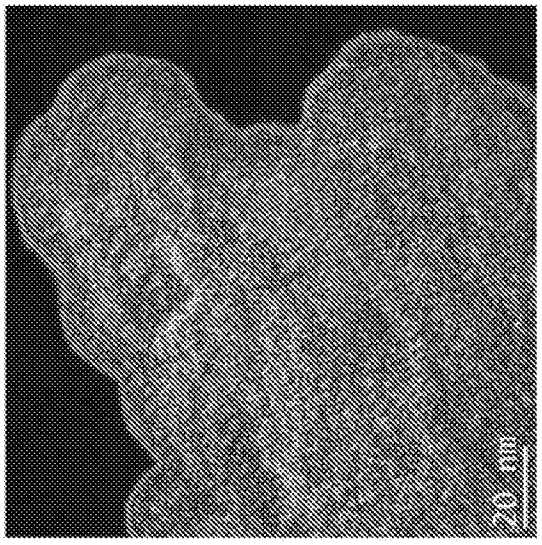

FIG. 1.2C

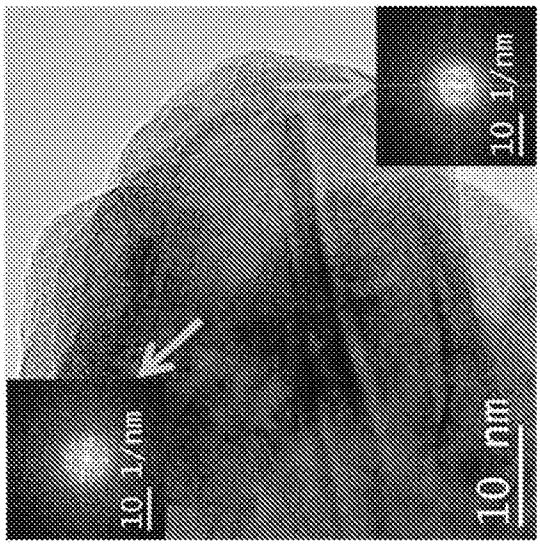

FIG. 1.2B

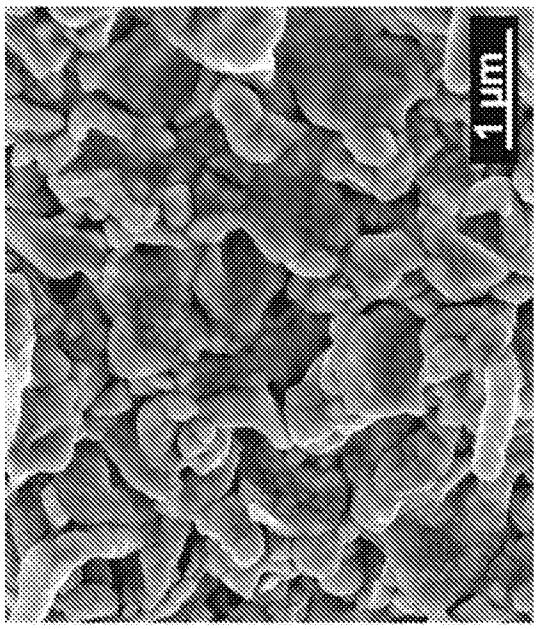

FIG. 1.2A

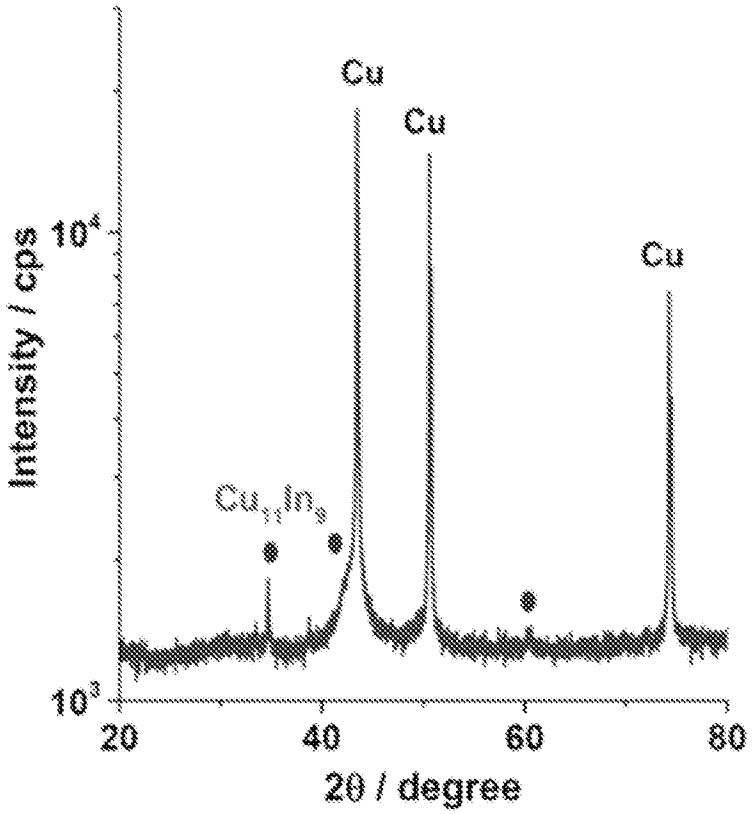

FIG. 1.3A

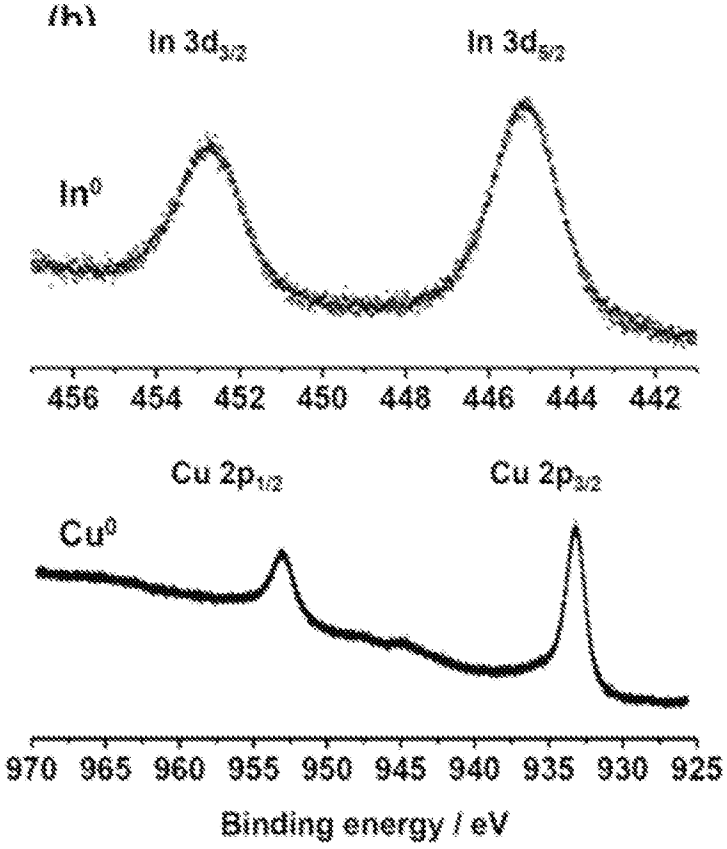

FIG. 1.3B

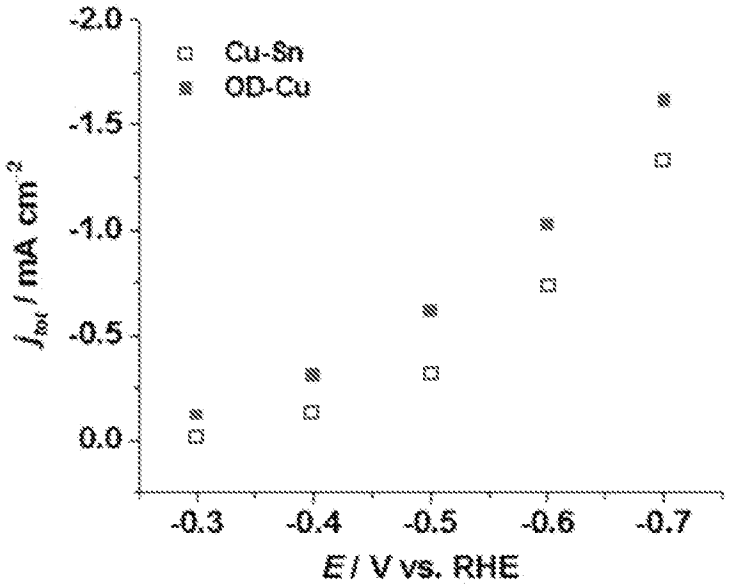

FIG. 1.4A

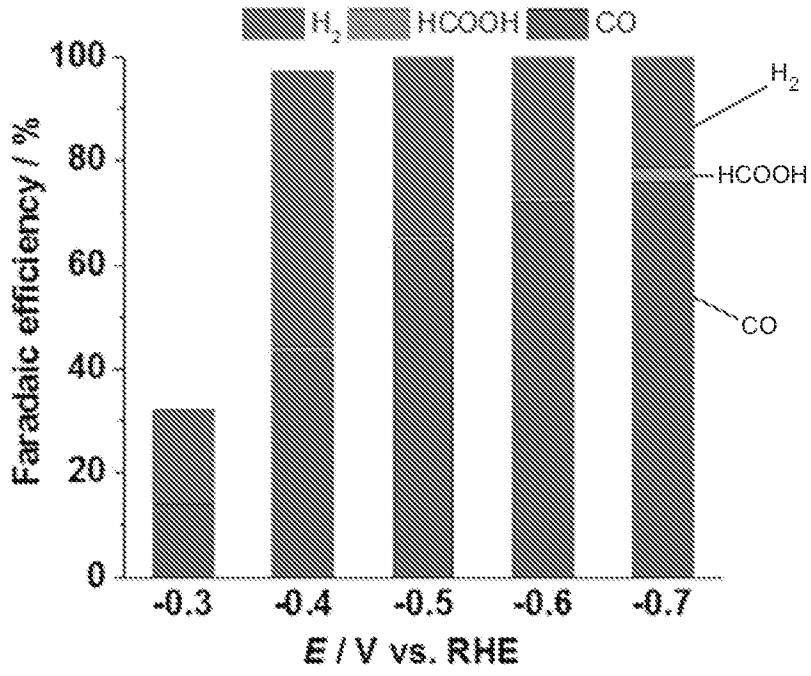

FIG. 1.4B

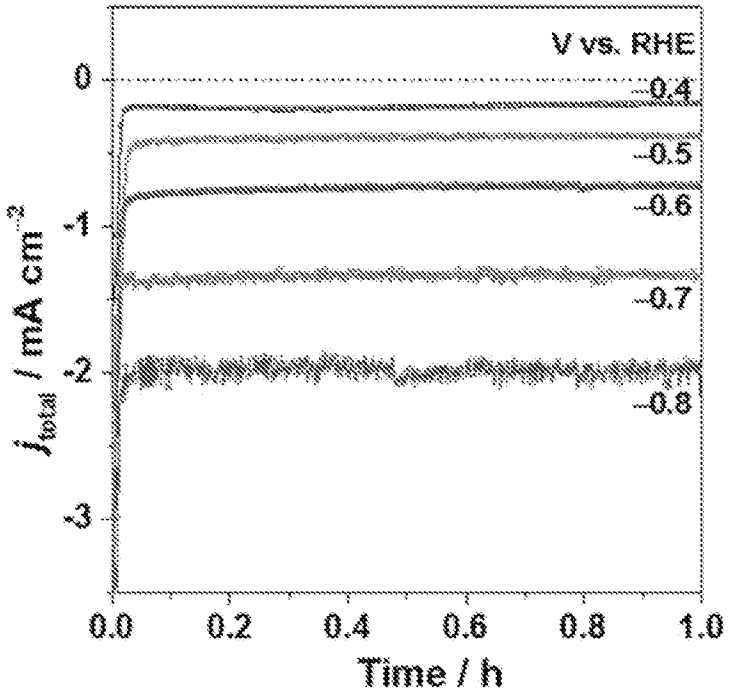

FIG. 2.1A

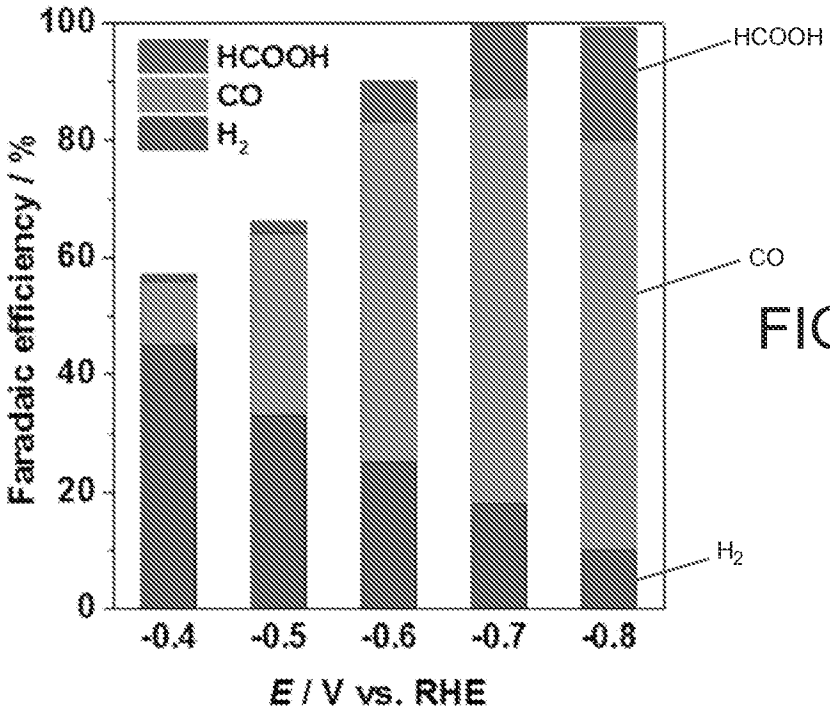

FIG. 2.1B

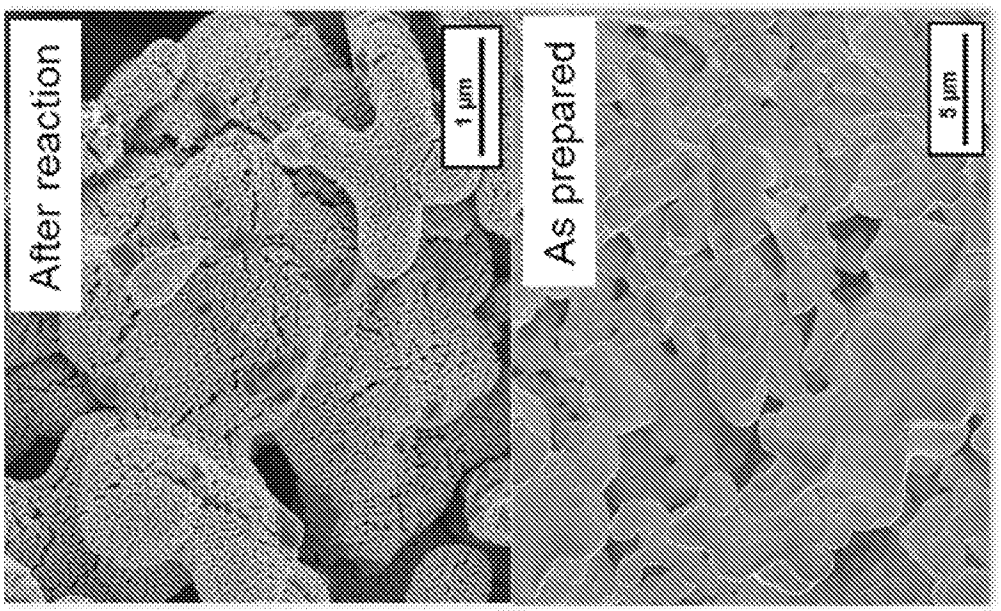

FIG. 2.2B

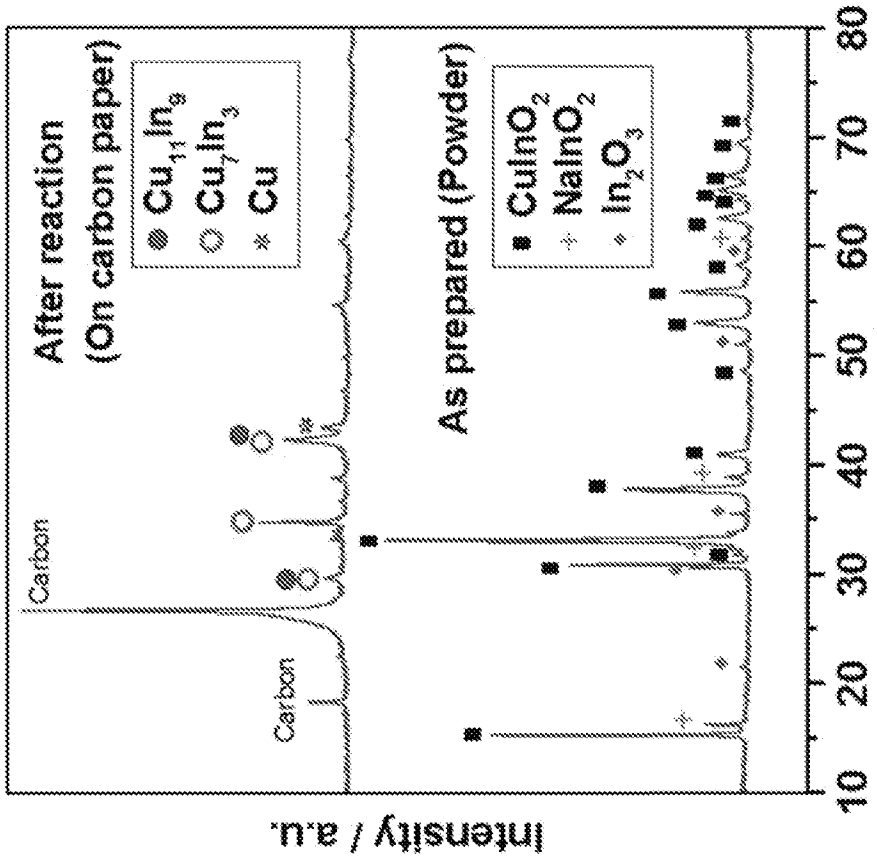

FIG. 2.2A

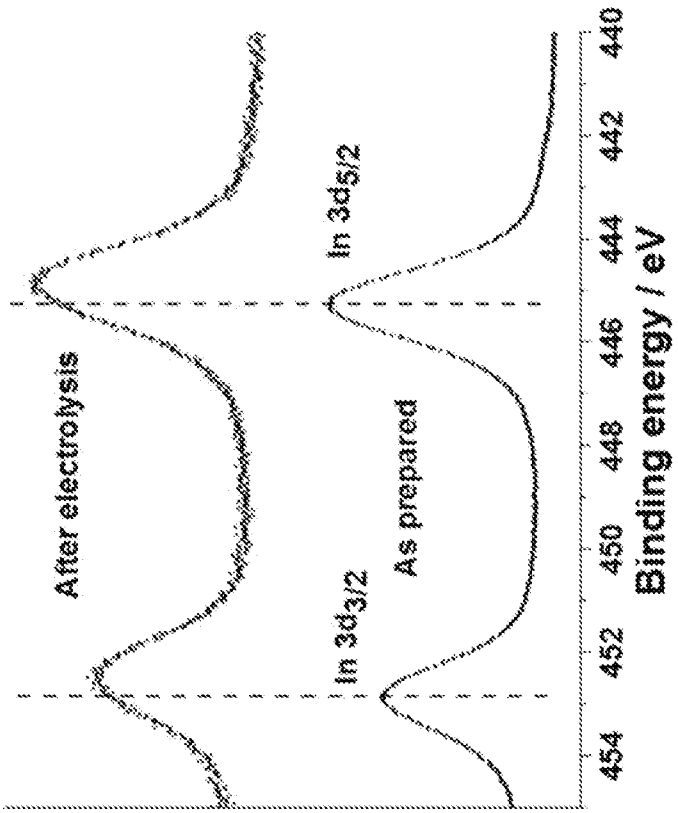

FIG. 2.3B

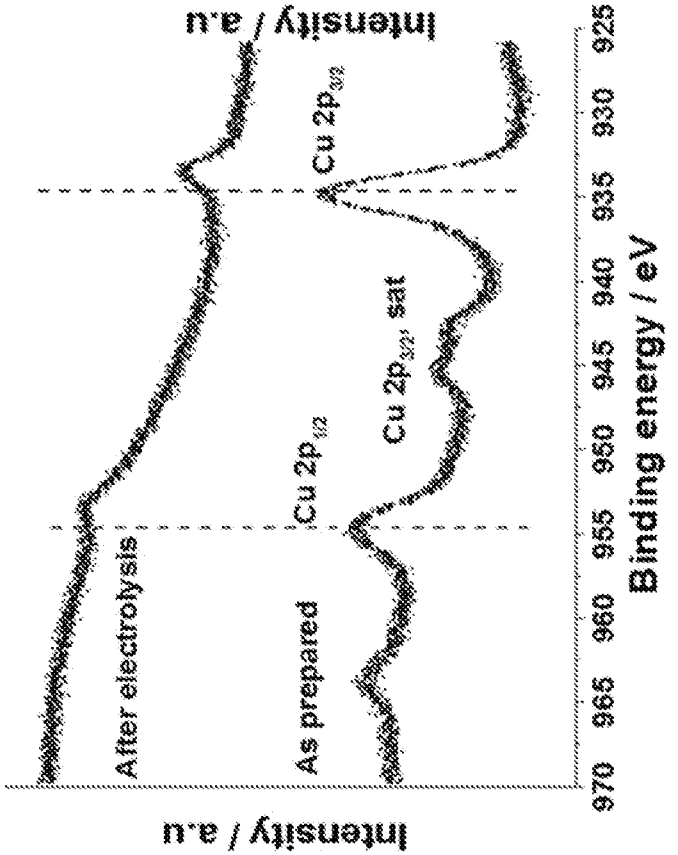

FIG. 2.3A

INTERNATIONAL SEARCH REPORT

International application No
PCT/IB2015/001687

A. CLASSIFICATION OF SUBJECT MATTER
INV. C25B11/04 C25B3/04
ADD.

According to International Patent Classification (IPC) or to both national classification and IPC

B. FIELDS SEARCHED

Minimum documentation searched (classification system followed by classification symbols)
C25B

Documentation searched other than minimum documentation to the extent that such documents are included in the fields searched

Electronic data base consulted during the international search (name of data base and, where practicable, search terms used)
EPO-Internal, WPI Data

C. DOCUMENTS CONSIDERED TO BE RELEVANT

Category*	Citation of document, with indication, where appropriate, of the relevant passages	Relevant to claim No.
X	US 2012/277465 A1 (COLE EMILY BARTON [US] ET AL) 1 November 2012 (2012-11-01) paragraph [0016] - paragraph [0018]; claims 1,2,4	1-3,6-8, 11-13
X	DATABASE WPI Week 201419 Thomson Scientific, London, GB; AN 2014-E13278 XP002751681, & WO 2014/034004 A1 (PANASONIC CORP) 6 March 2014 (2014-03-06) the whole document	1-3,5-8, 10-13,15

-/--

[X] Further documents are listed in the continuation of Box C.

[X] See patent family annex.

* Special categories of cited documents :

"A" document defining the general state of the art which is not considered to be of particular relevance

"E" earlier application or patent but published on or after the international filing date

"L" document which may throw doubts on priority claim(s) or which is cited to establish the publication date of another citation or other special reason (as specified)

"O" document referring to an oral disclosure, use, exhibition or other means

"P" document published prior to the international filing date but later than the priority date claimed

"T" later document published after the international filing date or priority date and not in conflict with the application but cited to understand the principle or theory underlying the invention

"X" document of particular relevance; the claimed invention cannot be considered novel or cannot be considered to involve an inventive step when the document is taken alone

"Y" document of particular relevance; the claimed invention cannot be considered to involve an inventive step when the document is combined with one or more other such documents, such combination being obvious to a person skilled in the art

"&" document member of the same patent family

Date of the actual completion of the international search	Date of mailing of the international search report
1 December 2015	15/12/2015

Name and mailing address of the ISA/	Authorized officer
European Patent Office, P.B. 5818 Patentlaan 2 NL - 2280 HV Rijswijk Tel. (+31-70) 340-2040, Fax: (+31-70) 340-3016	Hammerstein, G

1

Form PCT/ISA/210 (second sheet) (April 2005)

C(Continuation). DOCUMENTS CONSIDERED TO BE RELEVANT

Category*	Citation of document, with indication, where appropriate, of the relevant passages	Relevant to claim No.
X	US 2013/105304 A1 (KACZUR JERRY J [US] ET AL) 2 May 2013 (2013-05-02) paragraph [0068] - paragraph [0070]; claims 1-4	1,3-6, 8-11, 13-15
X	US 8 388 818 B1 (MENEZES SHALINI [US]) 5 March 2013 (2013-03-05) column 5, lines 40-44; claim 1	6-9, 11-14
X	JING LUO ET AL: "Facile one-step electrochemical fabrication of a non-enzymatic glucose-selective glassy carbon electrode modified with copper nanoparticles and graphene", MICROCHIMICA ACTA ; AN INTERNATIONAL JOURNAL ON MICRO AND TRACEANALYSIS, SPRINGER-VERLAG, VI, vol. 177, no. 3 - 4, 17 April 2012 (2012-04-17), pages 485-490, XP035055383, ISSN: 1436-5073, DOI: 10.1007/S00604-012-0795-4 the whole document	11,15

INTERNATIONAL SEARCH REPORT

Information on patent family members

International application No
PCT/IB2015/001687

Patent document cited in search report	Publication date	Patent family member(s)	Publication date
US 2012277465 A1	01-11-2012	AU 2012278949 A1	16-01-2014
		CA 2841062 A1	10-01-2013
		CN 103649374 A	19-03-2014
		EP 2729601 A1	14-05-2014
		JP 2014518335 A	28-07-2014
		KR 20140050038 A	28-04-2014
		US 2012277465 A1	01-11-2012
		US 2014027303 A1	30-01-2014
		WO 2013006711 A1	10-01-2013
WO 2014034004 A1	06-03-2014	JP 5636139 B2	03-12-2014
		US 2014360883 A1	11-12-2014
		WO 2014034004 A1	06-03-2014
US 2013105304 A1	02-05-2013	US 2013105304 A1	02-05-2013
		US 2013180863 A1	18-07-2013
		US 2014367273 A1	18-12-2014
US 8388818 B1	05-03-2013	NONE	